JOURNAL OF GUIDANCE, CONTROL, AND DYNAMICS
Vol. 28, No. 5, September–October 2005

Near-Optimal Low-Thrust Earth–Mars Trajectories via a Genetic Algorithm

Bradley Wall* and Bruce A. Conway†
University of Illinois at Urbana–Champaign, Urbana, Illinois 61801

A genetic algorithm is used to determine several types of Earth–Mars trajectories, with the objective of maximizing payload delivered to Mars. The trajectories have three phases: Earth escape, heliocentric flight, and arrival into low Martian orbit. The actual planetary orbits are used with one approximation: Mars's very small orbit inclination to the ecliptic plane is ignored. Impulses provided by chemical rockets are used for Earth departure and capture into orbit about Mars. The optimizer chooses the magnitude and direction of the impulse explicitly for the departure from Earth and implicitly, by choosing the hyperbolic excess velocity vector, for the arrival at Mars. The heliocentric flight uses low-thrust nuclear–electric propulsion; cases with continuous thrust and cases in which a coasting, that is, a no-thrust phase, is allowed are both considered. The continuous time history of the thrust pointing angle is modeled using a sequence of cubic polynomials whose coefficients become parameters of the genetic algorithm's chromosome. The fitness function of the genetic algorithm is dynamic; it first forces the spacecraft to arrive within the Martian sphere of influence. With that accomplished, it then emphasizes optimizing final mass.

Nomenclature

a	=	semimajor axis of an orbit
c_i	=	effective engine exhaust velocity of the ith stage
e	=	eccentricity of an orbit
g	=	Earth's gravity constant, 9.806 m/s
I_{sp}	=	specific impulse of the electric engine
ℓ	=	mean longitude of an orbit, $\varpi + M$
M	=	mean anomaly of an orbit, $n \cdot t$
m_{payload}	=	mass of payload delivered into Mars orbit
m_{power}	=	mass required for nuclear power producing unit
$m_{\text{propellant}\,i}$	=	spacecraft propellant mass for ith stage
$m_{\text{structure}\,i}$	=	spacecraft structural mass for ith stage
m_{thruster}	=	mass required for thrusters and supporting subsystems
m_0	=	initial spacecraft mass, 18,000 kg
$\dot{m}$	=	mass flow rate of electric engine
n	=	mean motion of an orbit, $\sqrt{\mu/a^3}$
P	=	power provided to electric engine
P_1	=	equinoctial element, $e \cdot \sin(\varpi)$
P_2	=	equinoctial element, $e \cdot \sin(\varpi)$
R	=	perturbing acceleration in the radial direction
r_{sc}	=	radial distance from the sun to the spacecraft
r_{SOI}	=	radius of the Mars sphere of influence
$r_{\infty/\text{Mars}}$	=	spacecraft radial distance from Mars following heliocentric flight
T	=	perturbing acceleration in the tangential direction
T_a	=	thrust acceleration magnitude
T_{eff}	=	electric engine efficiency
t	=	time
t_f	=	heliocentric time of flight
ti	=	time increment
t_{on}	=	length of time that the low-thrust electric engine is on
$V_{\infty/\text{Earth}}$	=	hyperbolic excess velocity
$V_{\infty/\text{Mars}}$	=	velocity of spacecraft with respect to Mars velocity
β	=	thrust pointing angle
Δm_i	=	mass required for the ith stage
ΔV_i	=	velocity change produced by the ith stage
ε	=	structural coefficient of spacecraft stage
θ	=	angle of hyperbolic excess velocity with respect to Earth's velocity
μ	=	gravitational constant for central body of a system
Ω	=	longitude of the ascending node of an orbit
ω	=	argument of periapsis of an orbit
ϖ	=	longitude of periapsis of an orbit, $\Omega + \omega$

Introduction

LOW-THRUST engines, that is, engines with thrust accelerations of less than 0.01 g, have recently begun to prove their usefulness for spacecraft propulsion. The successful Deep Space 1 spacecraft was the first to use this technology as its primary propulsion system. Launched on 24 October 1998, it was designed to test new technologies including a low-thrust xenon ion propulsion system. The engine operated for 677 days. By operating continuously, often for many months, low-thrust engines accelerate a spacecraft to the same final velocity as a chemical rocket engine. When low-thrust engines are used for a spacecraft trajectory, a continuous control history, that of the thrust pointing angle, is introduced. When numerical optimization is used to determine the optimal control, the methods used, whether direct or indirect, require good initial guesses to converge to a solution.[1] In contrast, a genetic algorithm (GA), as used here, uses the evolutionary ideas of selection, crossover, and mutation to evolve from a completely random population of initial guesses to a near-optimal solution, that is, a solution that may be optimal but does not satisfy analytic necessary conditions.[2]

GAs have previously been used to optimize low-thrust interplanetary trajectories. In research by Rauwolf and Coverstone-Carroll[3] the object was to reproduce closely the analytical solution used as an example in a text by Bryson and Ho[4] for a transfer from Earth orbit about the sun to Mars orbit about the sun. A model with circular Earth and Mars orbits was considered. The control used employed 10 discrete thrust pointing angles, equally spaced in time. Rauwolf and Coverstone-Carroll were able to find a near-optimal low-thrust trajectory solution qualitatively similar to the example in Ref. 4. Using an advanced GA operator called a micro-GA, Coverstone-Carroll[5] considered the same problem. Using both equality and inequality constraints on the terminal conditions, Coverstone-Carroll

Received 9 July 2004; revision received 23 December 2004; accepted for publication 23 December 2004.

*Graduate Research Assistant, Department of Aerospace Engineering.
†Professor, Department of Aerospace Engineering; bconway@uiuc.edu. Associate Fellow AIAA.

compared results with a traditional GA with one that included the micro-GA operator. Improved results were shown when the micro-GA operator was used with inequality constraints.

Tang and Conway[6] considered a low-thrust Earth-to-Mars transfer, including Earth departure and Mars arrival orbits. This was done using a patched-conic approximation connecting three phases of flight: Earth-centered low-thrust escape, heliocentric flight with continuous thrust, and Mars arrival and orbit circularization. A direct collocation method was used to solve the optimization problem for minimum time to Martian orbit. Coplanar circular orbits for Earth and Mars were assumed. Tang and Conway reported difficulty in finding an initial guess that converged to a globally optimal solution.

Problem Statement

The problem considered is optimization of an Earth–Mars trajectory including three phases: Earth escape, a low-thrust heliocentric trajectory, and Mars arrival. The objective of this work is to demonstrate the suitability of the GA method for finding approximate optimal interplanetary trajectories for a realistic model. Note that the problem can certainly be treated with extant, highly accurate methods. In fact, a qualitatively similar problem is solved, using collocation and nonlinear programming, by Tang and Conway.[6] The advantage of the GA approach is that it is simpler to implement and, unlike the more accurate methods, requires no a priori information about the optimal trajectory.

The goal of the trajectory optimization is to maximize payload delivered from low Earth orbit (LEO) to low Mars orbit (LMO). It is assumed that the spacecraft has an initial mass of 18,000 kg in a circular LEO with an altitude of 350 km. The orbit and mass reflect the performance of a current Delta IV rocket.[7] Impulses from rocket engines having an I_{sp} of 408 are used for Earth departure and LMO insertion. The LMO is assumed to be at an altitude of 500 km. Low-thrust electric engines are used during the heliocentric trajectory. Each of the empty stage masses is jettisoned after use. The patched conic method is used to join the three phases. The GA optimizer is allowed to find the best launch date, the magnitude and direction of the departure impulse, the heliocentric time of flight, the thrust pointing angle time history of the low-thrust engine during heliocentric flight, and the timing and duration of a heliocentric coast arc if one is optimizing. Eccentric Earth and Mars orbits are used with planetary positions found using an ephemeris.[8] However, it is assumed that the orbits of Earth and Mars are coplanar, that is, inclination is zero; this is not a bad assumption because the orbits are inclined by only $1^\circ 51'$.

Current technology estimates for mass required for the vehicle structure, that is, for the structural coefficient, and for all of the equipment, for example, the power-producing unit, required by the electric propulsion system are used.[9–11] The low-thrust engine used is a combination of 10 xenon ion thrusters with a specific impulse I_{sp} of 4110s and requiring a total constant power P of 69.9 kW (Ref. 10). A nuclear reactor power source is assumed to produce constant power P to the engine. The mass of the power system is assumed proportional to the power required, that is, it is determined as 26.4 (kg/kW) $\cdot P$ (Ref. 11). For 69.9 kW of required power, this gave a mass of 1845 kg for the power system. Masses for the thrusters themselves, as well as the supporting systems, including the tank holding the xenon propellant, the tubing substructure, and the supporting structure, are also assumed to have a total mass proportional to the power required,[11] as 2.5 (kg/kW) $\cdot P$. This provided a mass of 175 kg for the thrusters and supporting substructures, resulting in a total structural mass of 2020 kg for the electric propulsion system. Optimal trajectories are found for several assumed low-thrust engine efficiencies, from 68 to 80%, where efficiency is defined as the ratio of thrust produced to the theoretical maximum thrust, $(2 \cdot P)/(I_{sp} \cdot g)$.

Governing Equations

The time rate of change equations for the Keplerian, or classical, orbital elements e, Ω, and ω have singularities at an inclination of zero and at an eccentricity of zero. These conditions would cause difficulty in the numerical integration because there is no orbit inclination and the transfer orbit initially has very little eccentricity, approximately equal to that of Earth's orbit, 0.0167 (Ref. 9).

To avoid this problem, two equinoctial elements, P_1 and P_2, introduced by Lagrange, are used (see Ref. 12). The angular orbital element used is the mean longitude ℓ. The time rates of change equations for semimajor axis a, elements P_1, P_2, and ℓ as functions of radial and tangential thrust accelerations R and T, respectively, are due to Battin.[12] The final equation of motion defines the time variation of thrust acceleration:

$$\frac{\mathrm{d}}{\mathrm{d}t}T_a = \frac{T_a^2}{c} \tag{1}$$

where T_a is the magnitude of the thrust acceleration and c is the effective engine exhaust velocity. The radial and tangential components of the thrust acceleration are then determined by the thrust pointing angle, that is,

$$R = T_a \cdot \sin\beta \tag{2}$$

$$T = T_a \cdot \cos\beta \tag{3}$$

So that the numerical values for the time rates of change of all five variables, a, P_1, P_2, ℓ, and T_a, remain small, a new set of canonical units is introduced. The semimajor axis is expressed in a distance unit (DU) equivalent to the astronomical unit (AU) of 1.496×10^8 km. The sun's gravitational constant μ is defined as $1\mathrm{DU}^3/\mathrm{TU}^2$, so that the period of a circular orbit at 1 DU is 2π time units (TU). Thus, 1 TU = 58.135 days. The use of these units makes all of the state variables and their time rates of change approximately the same order of magnitude. This makes for efficient numerical integration of the system variational equations by the ordinary differential equations (ODE) subroutine.[13]

GA Parameters

The heliocentric trajectory includes a continuous thrust pointing angle time history. Tang and Conway[6] showed that the optimal thrust pointing angle for a heliocentric flight could be represented using a single cubic polynomial. However, to better approximate the thrust pointing angle time history, a sequence of three cubic polynomials placed end to end is used in this work. To maintain simplicity, only the two cubic polynomials at the beginning $[\beta_1(t)]$ and end $[\beta_3(t)]$ were chosen by the GA. The eight coefficients required were GA parameters. The third cubic $[\beta_2(t)]$ connects these two cubic polynomials. This third cubic is constrained to be continuous in value and in slope, and so it is determined from the terminal condition of $\beta_1(t)$ and the initial condition of $\beta_3(t)$, that is, it is found only implicitly by the GA.

The heliocentric flight phase was divided into 100 time increments ti. The cubic for $\beta_1(t)$ is centered at time step 24 and the cubic for $\beta_3(t)$ at time step 76. The cubic for $\beta_2(t)$ spans from time step 48 to 52. This produced a completely continuous thrust pointing angle time history using only eight GA optimization parameters. Figure 1 shows an example thrust pointing angle time history by using the following equations:

$$\beta_1(t) = a_1 \cdot (t - 24 \cdot ti)^3 + a_2 \cdot (t - 24 \cdot ti)^2 + a_3 \cdot (t - 24 \cdot ti) + a_4 \tag{4}$$

$$\beta_2(t) = b_1 \cdot t^3 + b_2 \cdot t^2 + b_3 \cdot t + b_4 \tag{5}$$

$$\beta_3(t) = c_1 \cdot (t - 76 \cdot ti)^3 + c_2 \cdot (t - 76 \cdot ti)^2 + c_3 \cdot (t - 76 \cdot ti) + c_4 \tag{6}$$

The cubic coefficients were bounded so that the thrust pointing angle was bounded between $\pm\pi$ (Table 1).

In this test, near-optimal trajectories were obtained for three cases, a no-coast case in which the thrust is always on; a one-coast case in which the thrust is on for some span of time following Earth departure, then turned off for a span of time, and then turned on again

Table 1 GA inputs for all three cases[a]

No.	Parameter	Lower bound	Upper bound	Possibilities	Resolution
1	Time of flight t_f, day	1	512	512	1
2	Time of launch, day	0	1023	1024	1
3	θ, rad	0	$\pi/2$	4	$\pi/6$
4	$V_{\infty/\text{Earth}}$, DU/TU	0	0.03	4	0.01
5	First cubic coefficient a_1				
6	First cubic coefficient a_2				
7	First cubic coefficient a_3	$-\pi$ /			
8	First cubic coefficient a_4	$[(0.24*t_f)^3$	π /$[(0.24*t_f)^3$		
9	Third cubic coefficient c_1	$+(0.24*t_f)^2$	$+(0.24*t_f)^2$	32	N/A
10	Third cubic coefficient c_2	$+0.24*t_f+1]$	$+0.24*t_f+1]$		
11	Third cubic coefficient c_3				
12	Third cubic coefficient c_4				
13	Time of first thrusting arc, day	1	128	128	1
14	Time of second thrusting arc, day	1	128	128	1
1a	Time of flight t_f, day	1	512	512	1
2a	Time of launch, day	0	1023	1024	1
3a	θ, rad	0	$\pi/2$	4	$\pi/6$
4a	$V_{\infty/\text{Earth}}$, DU/TU	0.001	0.256	256	0.001

[a]Parameter inputs for the no-coast (1–12) cases, one-coast cases (1–14), and two-impulse cases (1a–4a).

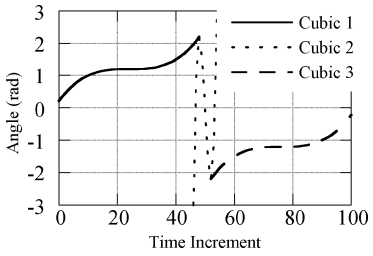

Fig. 1 Example of continuous thrust pointing angle produced from three cubic polynomials.

until Mars is reached; and a conventional two-impulse case, that is, using no low-thrust propulsion, only one impulse for Earth departure and one for LMO insertion. Trajectories for the one-coast case were obtained because a trajectory including a coasting arc was believed to be beneficial. All cases include a GA optimization parameter time of flight representing the heliocentric flight time. The one-coast case included two additional parameters, length of first thrusting arc and length of second thrusting arc. These parameters were chosen because it was likely that they would vary independently of the parameter time of flight. This parameter-independent behavior is beneficial to a GA optimizer.

Fitness Function

The fitness function is an integral part of the GA. The definition of this function, by which every individual was evaluated, had two objectives: 1) to assure feasible trajectories, those in which the spacecraft is within the sphere of influence (SOI) of Mars after the heliocentric phase; and 2) to maximize payload mass into LMO. The following equations defined the fitness function used to accomplish this:

$$\text{If } r_{\infty/\text{Mars}} < r_{\text{SOI}}, \text{ then fitness} = -\left[(m_0 - m_{\text{payload}})/m_0\right] \quad (7)$$

$$\text{else fitness} = -\left[(m_0 - m_{\text{payload}})/m_0\right] + \left[(r_{\infty/\text{Mars}} - r_{\text{SOI}})/r_{\text{SOI}}\right] \quad (8)$$

where m_0 is the initial spacecraft mass and $r_{\infty/\text{Mars}}$ and r_{SOI} are the position of the spacecraft with respect to Mars at the end of the heliocentric flight phase and the radius of the Martian SOI, respectively, both in units of Martian radii.[9] The GA attempts to maximize the fitness function. Clearly, the position term will dominate at first, forcing the GA to find trajectories that end within the SOI of Mars. Note that all possible trajectories have a fitness greater than -1.

A random number generator determined the initial population, that is, no initial guess is required. The total length of the chromosome is 63 binary digits for the no-coast case and 77 for the one-coast case. Numerical experiments with varying population sizes, between 50 and 300 individuals, crossover probabilities between 30 and 80%, and mutation probabilities between 0.1 and 0.5% were tried. However, the best results were obtained using a population of 150 individuals and probabilities of crossover and mutation of 50 and 0.5%, respectively.

Payload values within 10% of the solution after 15,000 generations were obtained after just a few hundred generations, but it was desired to see a GA solution show no improvement for at least 1000 generations before the solution was accepted as a near-optimal solution.

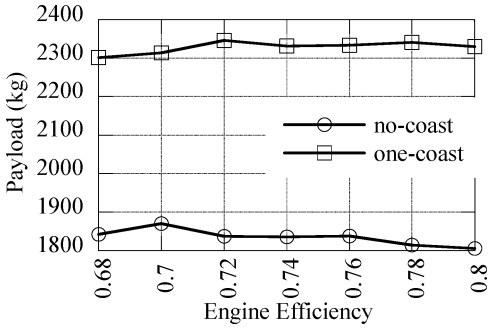

Fig. 2 Payload comparison for all low-thrust cases.

Results

In this section we compare the payload mass delivered to Mars for the three cases considered; no-coast, one-coast, and (conventional) two-impulse case. We also note the similarities and differences in the respective trajectories and thrust pointing angle time histories. Table 2 presents a direct comparison of the no-coast and one-coast cases (at engine efficiencies of 0.68 and 0.80). Table 2 also includes, in its fifth column, a direct comparison to the two-impulse transfer.

A comparison of the payload mass delivered into Martian orbit between the no-coast and one-coast cases shows an approximately 500-kg increase in payload for the one-coast cases vs the comparable no-coast cases (Fig. 2). This payload increase is almost entirely due to propellant mass saved during the heliocentric phase. The two-impulse trajectory yields the greatest payload, 2694 kg. Whereas the addition of the low-thrust engines to the heliocentric trajectory saved a significant amount of mass in phase 3, that is, Mars arrival, compared to the two-impulse case, it did not offset the cost of the mass of the power system and substructure used during the heliocentric trajectory, 2020 kg. Therefore, implementing a low-thrust trajectory is only optimal if the low-thrust engine is used for two or all three phases of the trajectory, that is, Earth arrival, heliocentric flight, and Mars arrival.

Table 2 Comparison of the no-coast and one-coast low-thrust trajectories with the two-impulse solution

Case	One-coast	No-coast	One-coast	No-coast	Two-impulse
Power/engine, W	6,990	6,990	6,990	6,990	N/A
I_{sp}, s	4,110	4,110	4,110	4,110	N/A
T_{eff}	0.68	0.68	0.80	0.80	N/A
$\dot{m}$/engine, kg/s	5.85$E-$06	5.85$E-$06	6.88$E-$06	6.88$E-$06	N/A
c_1, km/s	4	4	4	4	4
c_2, km/s	40.31	40.31	40.31	40.31	N/A
c_3, km/s	4	4	4	4	4
Total thrust, N	2.36	2.36	2.77	2.77	N/A
ΔV_1, km/s	3.19	3.22	3.19	3.22	3.43
ΔV_2, km/s	4.87	8.33	5.26	9.23	N/A
ΔV_3, km/s	1.48	1.68	1.40	1.63	2.43
Total ΔV, km/s	9.54	13.24	9.85	14.08	5.86
Time to launch, days	352	384	352	384	373
Time of flight t_f, days	304	232	321	216	252
Time of arrival, days	656	616	673	600	625
Coast trajectory, days	161	0	190	0	252
Thrusting days, t_{on}	143	232	131	216	N/A
$V_{\infty/\text{Earth}}$, km/s	0.30	0.89	0.00	0.89	2.32
θ, deg	90	30	90	30	0
$V_{\infty/\text{Mars}}$, km/s	0.99	1.72	0.47	1.56	3.32
Δm_1, kg	11,643.30	11,720.52	11,633.58	11,720.52	12,200.82
Δm_2, kg	2,743.14	3,193.10	2,799.30	3,304.92	N/A
Δm_3, kg	1,312.36	1,244.22	1,236.97	1,168.90	3,105.52
Total Δm, kg	15,698.80	16,157.84	15,669.85	16,194.34	15,306.34
Initial T_a, g	3.78$E-$05	3.83$E-$05	4.44$E-$05	4.51$E-$05	N/A
m_{payload}, kg	2,301.20	1,842.16	2,330.15	1,805.66	2,693.66
$m_{\text{structure1}}$, kg	1,746.49	1,758.08	1,745.04	1,758.08	1,830.12
$m_{\text{propellant1}}$, kg	9,896.80	9,962.44	9,888.55	9,962.44	10,370.70
$m_{\text{structure2}}$, kg	2,020.11	2,020.11	2,020.11	2,020.11	N/A
$m_{\text{propellant2}}$, kg	723.00	1,172.99	779.21	1,284.81	N/A
$m_{\text{structure3}}$, kg	196.85	186.63	185.55	175.33	465.83
$m_{\text{propellant3}}$, kg	1,115.51	1,057.59	1,051.42	993.56	2,639.69
ε_1 and ε_3	0.15	0.15	0.15	0.15	0.15
ε_2	0.74	0.63	0.72	0.61	N/A
$r_{\infty/\text{Mars}}(r_{\text{Mars}})$	150.18	165.11	162.00	164.87	121.51
Flight angle flown through, deg	227.06	169.85	237.77	160.23	186.48

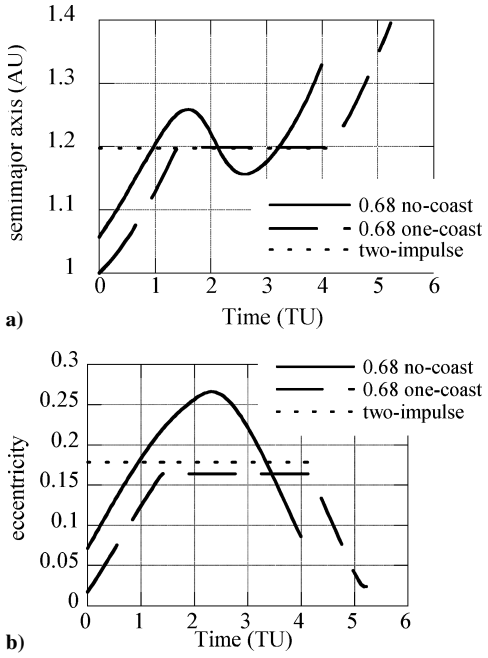

Fig. 3 Time histories of a) semimajor axis and b) eccentricity.

Note in Fig. 2 that there appears to be no relationship between payload mass and engine efficiency when one would logically conclude payload mass should increase with increasing engine efficiency. However, the results are similar, and only small percentage changes in the results would be required to yield the expected dependence. That is, it is likely that the small differences between the solutions obtained and the true optimal solutions are sufficient to conceal the expected small dependence of payload mass on engine efficiency.

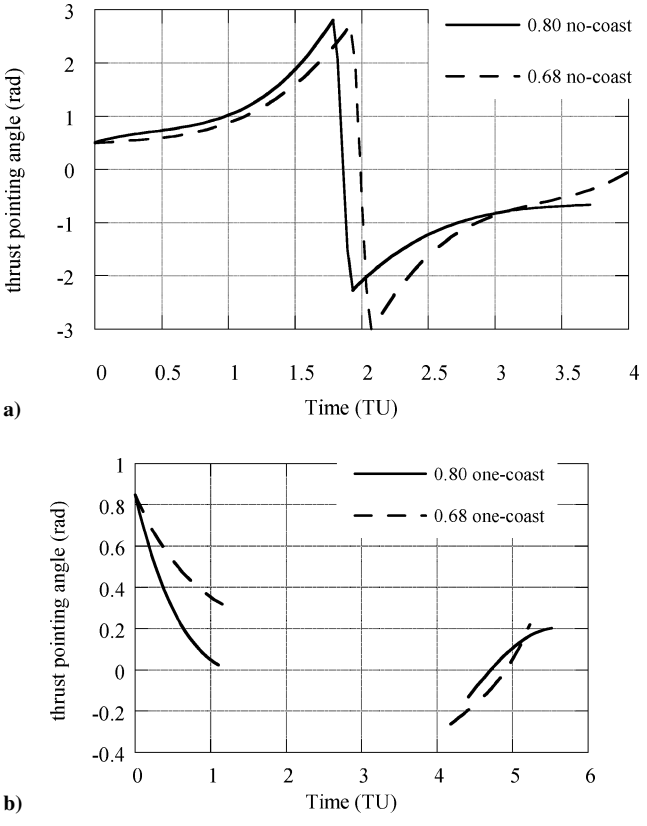

Fig. 4 Thrust pointing angle time history of two select a) no-coast and b) one-coast cases.

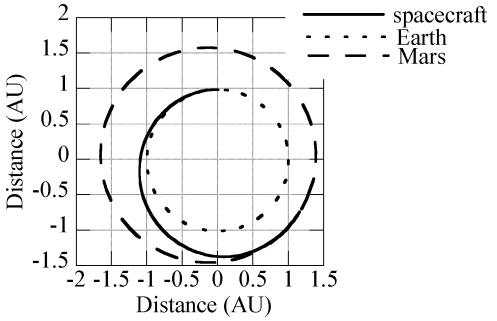

Fig. 5 Sample one-coast trajectory.

Figure 3 shows semimajor axis and eccentricity time histories for selected trajectories. Note the initial difference in semimajor axis and eccentricity between the no-coast and one-coast cases. This difference can be related to an observed difference in time to launch for these trajectories. The greater time-to-launch parameter for the no-coast trajectories causes the trajectory to begin closer to the aphelion of Earth's orbit. Because the spacecraft position must initially be equal to that of Earth and because all of the trajectories are initially similar, there is an observed initial increase in semimajor axis and eccentricity, 0.057 AU and 0.055, respectively. It is also observed that the time rates of change for the semimajor axis and eccentricity on the initial and terminal arcs are similar for both the one-coast and no-coast trajectories, despite the qualitatively different thrust pointing angle time histories (Fig. 4). Note that the time rates of change of the semimajor axis and eccentricity increase for increasing engine efficiencies. Figure 5 shows a sample one-coast trajectory found by the GA.

Conclusions

The GA is capable of optimizing a Mars mission of respectable fidelity, that is, one including a departure from LEO and arrival into Martian orbit and using ephemerides to locate the planets as a function of time. The GA generates reliable results; it creates similar trajectories with comparable payload masses for all of the no-coast and one-coast cases, respectively, as well as a two-impulse trajectory that is similar to a Hohmann transfer, that is, one in which the direction of $V_{\infty/\text{Earth}}$ is essentially parallel to Earths velocity and the flight angle flown through is close to 180 deg. The method of parameterizing a continuous control history by representing it as a sequence of polynomials in time works well and economizes on the number of GA parameters required. Note that the results presented are near-optimal solutions. However, these near-optimal solutions are sufficiently good that they could provide initial guesses for indirect or direct methods capable of more precise solutions.

Acknowledgments

The research was supported in part by NASA Grant NAG 3-2791, with John Riehl of NASA John H. Glenn Research Center at Lewis Field as Technical Monitor. The genetic algorithm was developed from "program gafortran version 1.7a" written by David Carroll.

References

[1]Enright, P. J., and Conway, B. A., "Discrete Approximations to Optimal Trajectories Using Direct Transcription and Nonlinear Programming," *Journal of Guidance, Control, and Dynamics*, Vol. 15, No. 4, 1992, pp. 994–1002.

[2]Goldberg, D., *Genetic Algorithms in Search, Optimization, and Machine Learning*, Addison Wesley Longman, Reading, MA, 1989, Chap. 1.

[3]Rauwolf, G., and Coverstone-Carroll, V., "Near-Optimal Low-Thrust Orbit Transfers Generated by a Genetic Algorithm," *Journal of Spacecraft and Rockets*, Vol. 33, No. 6, 1996, pp. 859–862.

[4]Bryson, A., and Ho, Y., *Applied Optimal Control: Optimization, Estimation and Control*, rev., Hemisphere, Washington, DC, 1975, pp. 66–69.

[5]Coverstone-Carroll, V., "Near-Optimal Low-Thrust Trajectories via Microgenetic Algorithms," *Journal of Guidance, Control, and Dynamics*, Vol. 20, No. 1, 1996, pp. 196–198.

[6]Tang, S., and Conway, B. A., "Optimization of Low-Thrust Interplanetary Trajectories Using Collocation and Nonlinear Programming," *Journal of Guidance, Control, and Dynamics*, Vol. 18, No. 3, 1995, pp. 599–604.

[7]"Delta IV Payload Planners Guide," URL: http://www.boeing.com/defense-space/space/delta/docs/DELTA_IV_PPG_2000.PDF, 2004.

[8]"Planetary Orbital Elements," URL: http://ssd.jpl.nasa.gov/elem_planets.html, 2004 [cited 3 March 2005].

[9]Prussing, J., and Conway, B., *Orbital Mechanics*, Oxford Univ. Press, New York, 1993, pp. 81–96 and 188–190.

[10]Patterson, M., Foster, J., Haag, T., Soulas, G., Pastel, M., and Roman, R., "Next: NASA's Evolutionary Xenon Thruster Development Status," AIAA Paper 2003-4862, July 2003.

[11]Mason, L. S., "A Comparison of Brayton and Stirling Space Nuclear Power Systems for Power Levels from 1 Kilowatt to 10 Megawatts," NASA TM 2001-210593, Jan. 2001.

[12]Battin, R. H., *An Introduction to the Mathematics and Methods of Astrodynamics*, AIAA, New York, 1987, pp. 492–494.

[13]Shampine, L. F., and Gordon, M. K., *Computer Solution of Ordinary Differential Equations: The Initial Value Problem*, Freeman and Co., San Francisco, 1975, Chap. 10.